

DASY8/6 Module WPT

PIA INQUIRY

Compliance Testing against SAR
and MPE Limits (V1.2 August 2025)



APPROVED

Revision History

Revision	Date	Author(s)	Description
1.0	09.05.2025	Jingtian Xi	Initial version
1.1	04.06.2025	Jingtian Xi	Added validation results and uncertainty budget
1.2	07.08.2025	Jingtian Xi	Added additional information after FCC approval (Section 2)

PIA Inquiry: Compliance Testing against SAR and MPE Limits with DASY8/6 Module WPT

1 Scope of the PIA Application

With this Persistent Inquiry Acceptance (PIA) submission, we seek acceptance by the US Federal Communications Commission (FCC) for the application of DASY8/6 Module WPT V2.8+ in demonstrations of the compliance of any wireless power transfer (WPT) device with respect to:

- Part 1: specific absorption rate (SAR) limits in the frequency range 100 kHz to 4 MHz as defined in Section 3
- Part 2: maximum permissible exposure (MPE) limits in the frequency range below 100 kHz as defined in Section 4

According to the guidance from the Telecommunication Certification Body (TCB) Workshop held in April 2025 (RF Exposure Session, Section 2), the PIA could be released to grant users of DASY8/6 Module WPT V2.8+ for compliance testing use without the need to file numerical simulation (NUMSIM) pre-approval guidance (PAG) documents.

2 FCC Approval

FCC's approval specifies the following:

Note: Any applicant for certification that leverages the technology discussed in this PIA will be required to supply the TCBs with a detailed description of the technology such that they will be able to review and establish that it meets the FCC requirements for the NUMSIM PAG exemption per KDB 388624-D02. That certification application must also include an attestation and technical document to be filed in the Operational Description of the EAS filings with the KDB inquiry number for the PIA itself; the KDB number is for the FCC to be able to track the PIA information associated with the EAS filing. It is then essential that whoever leverages this PIA would have KDB inquiry number as well.

In summary: Always attach an "ECR Information" exhibit with the PIA-approved KDB number 130303 when using DASY8/6 Module WPT V2.8+ following the method and procedure defined hereafter to enable TCB assessment and allow the FCC to track the waiver's approval.

3 Part 1: Evaluation of Compliance with SAR Limits from 100 kHz - 4 MHz

3.1 System Requirements

To determine the peak SAR averaged over a mass of 1 or 10 gram (psSAR1g/10g) as required by §1.1310 of the FCC rules [1] at frequencies of < 4 MHz, the following instrumentation is required:

- DASY8/6 Module WPT V2.8+ including:
 - MAGPy-8H3D+E3D Version 2 or Version 3 probe with the integrated data acquisition system MAGPy-DAS
 - MAGPy-RAϕV2 reference probe as a phase reference
 - MAGPy-ES emergency stop system
- WPT source V-Coil50/400 for system check and validation purposes
- Software DASY8/6 Module WPT V2.8+

3.2 System Performance Check

Execution of the system performance check before the psSAR1g/10g evaluation of the device under test (DUT) is recommended. The performance check is equivalent to an assessment of an unknown source for which the target values are known. A system performance check with the source V-Coil50/400 is considered successful if the difference between the SAR measurement result and the target value is smaller than the system check uncertainty of 25.6% for psSAR1g or 25.2% for psSAR10g.

3.3 Assessment of psSAR1g/10g

The workflow to demonstrate compliance of WPT devices with SAR limits operated in the frequency range from 100 kHz to 4 MHz is described below and is illustrated in Figure 1.1. More information about each step can be found in Section 7 of the system manual [2].

3.3.1 Volume Scan

In the volume scan, all three components of the magnetic (H-) field (i.e., H_x , H_y , and H_z) generated by the DUT are measured in a volume on top of and as close as physically possible to the DUT. The volume consists of measurement points distributed at uniform steps of 7.33 mm. The scan volume is large enough to include the entire incident field to which the standardized homogeneous phantom is exposed, i.e., the uncertainty with respect to the induced SAR inside the infinite half-space phantom can be assumed to be < 0.1 dB.

The peak frequency of the DUT is determined from the spectrum derived by application of a fast Fourier transformation (FFT) to the time-domain signal captured at the reference probe positioned next to the DUT. Zero padding and quadratic fit are applied to improve the resolution of the peak frequency determination. The amplitudes of H_x , H_y , and H_z at the peak frequency are determined by applying discrete Fourier transformation (DFT) of the time-domain signals captured at the corresponding H-field sensors. Phases of H_x , H_y , and H_z with respect to the reference probe at the peak frequency are retrieved from the complex-valued frequency-domain data.

With the electric (E-) field sensors integrated in the MAGPy probe, the amplitudes of all three components of the incident E-field (i.e., E_x , E_y , and E_z) are also measured in the volume scan.

3.3.2 Method of Extra- and Interpolation

The extra- and interpolation operations are both applied to the incident H-field. The extrapolation down to the probe tip (also called surface field reconstruction [2]) is achieved by reconstruction based on the curl- and divergence-free conditions of Maxwell's equations. The measured H-fields at the upper planes of the scan volume and the reconstructed H-fields at the bottom plane generally correspond to the measurement grid with a uniform step of 7.33 mm; these are tri-linearly interpolated to a fine grid with an approximately uniform step of 1 mm.

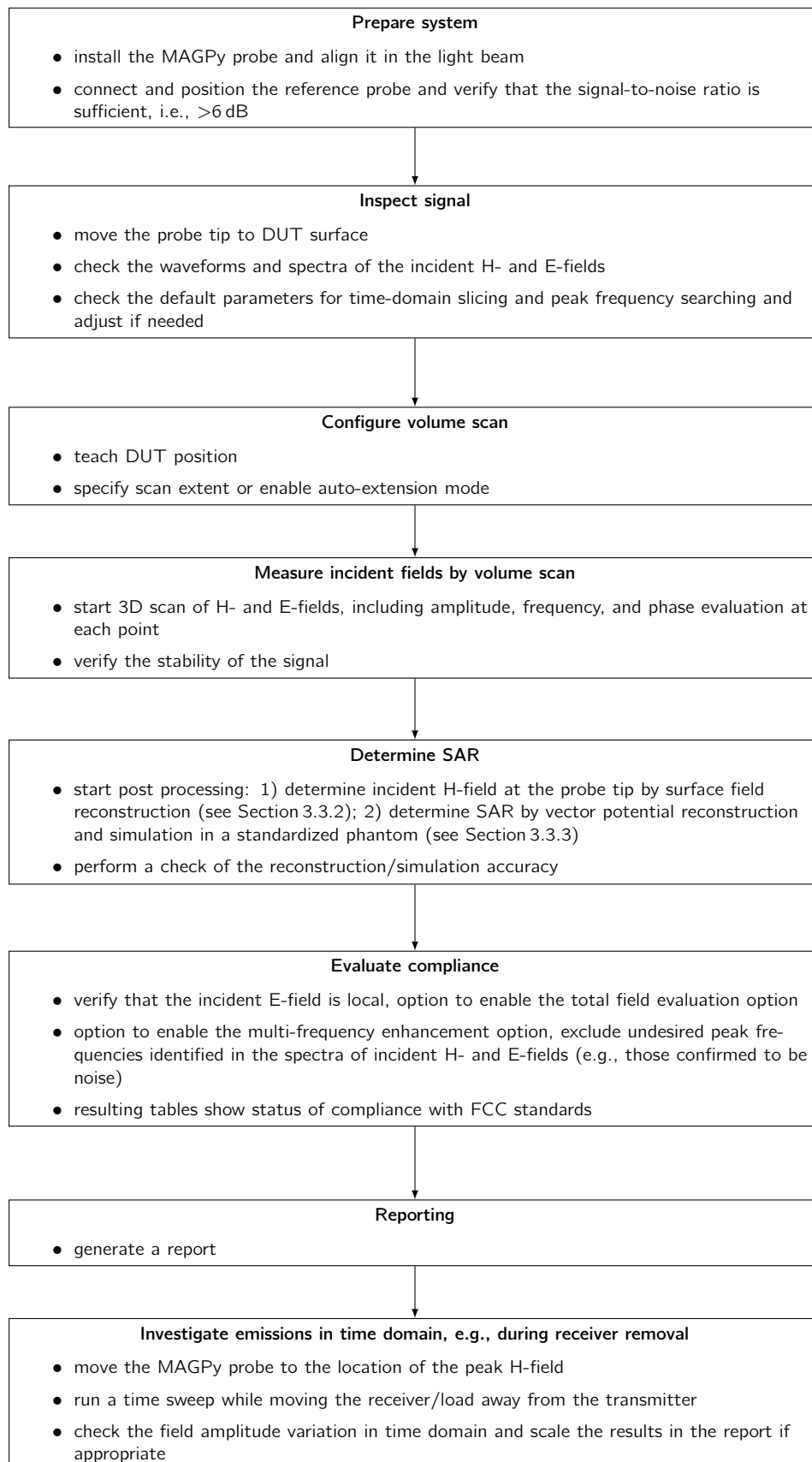


Figure 1.1: Measurement procedure for using DASY8/6 Module WPT V2.8+ to evaluate compliance of WPT devices with SAR limits over the frequency range 100 kHz – 4 MHz.

3.3.3 Method of Induced Field Determination

The determination of the induced E-field includes the following steps:

1. reconstruction of the vector potential (i.e., A-field) based on the measured and reconstructed H-field [3]
2. solution of the induced scalar potential ϕ with $\nabla \cdot \sigma \nabla \phi = -j\omega \nabla \cdot \sigma A$ via application of the finite element method (FEM) with linear nodal elements and zero-flux boundary conditions in the standardized homogeneous phantom ($\sigma = 0.75 \text{ S/m}$, $\rho = 1000 \text{ kg/m}^3$) [4]
3. computation of the induced E-fields with $E = -j\omega A - \nabla \phi$; the gradient $\nabla \phi$ is computed via the FEM element function's derivation and is evaluated at the center of the cell

The computation of the local SAR is based on the induced E-field ($\text{SAR} = \sigma E^2 / \rho$). The local SAR distribution is numerically integrated within the 1g or 10g volume, where the length of the side is $\sqrt[3]{1\text{g}/\rho}$ or $\sqrt[3]{10\text{g}/\rho}$ and the maximum value is reported as psSAR1g/10g.

3.3.4 Evaluation of Compliance

In the "Compliance (Field values)" table of the DASY8/6 Module WPT V2.8+ manual, the peak values of different field quantities according to the relevant safety standards or regulations are listed; this table facilitates the comparison of results with the safety limits. In the "Compliance (Ratios)" table, the exposure ratios – i.e., the ratios of the peak field values to the corresponding limit – are listed. This table also provides advanced evaluation options, i.e., the total field evaluation, including any exposure due to the incident E-field, and multi-frequency evaluation equivalent to a total-exposure-ratio calculation so that exposures at non-negligible secondary peak frequencies are covered.

3.3.5 Reporting

The report delivered by DASY8/6 Module WPT V2.8+ provides information about the DUT, the software and probe used in the measurement, the volume scan configuration, visualization of the H-field spectrum, and the incident H- and E-field measurements, as well as tables summarizing the peak field values and the exposure ratios for relevant safety standards or regulations.

3.3.6 Time-Domain Evaluation

The highest exposure from a WPT transmitter (e.g., a wireless charger) may take place during the removal of the receiver (e.g., a mobile phone being charged). The time sweep (i.e., zero span) function of DASY8/6 Module WPT V2.8+ enables measurement of the H-field amplitude as a function of time and can be used to investigate the field variation during removal of the receiver. The evaluation results can be scaled according to the field increase captured.

3.4 System Check Uncertainty

The uncertainty in the system check for SAR assessments performed with DASY8/6 Module WPT V2.8+ according to the described procedure was determined following IEC/IEEE 63184 [4] and documented in the system manual [2], whereby the uncertainty in the calibration is reduced to the uncertainty in repeatability, and the isotropic uncertainty is reduced due to the well-defined orientation of the probe to the coil. The detection limit uncertainty is set to zero due to the high signal-to-noise ratio of the source.

System Check Uncertainty Budget for psSAR1g according to IEC/IEEE 63184						
Item	Error Description	Uncertainty Value (\pm dB)	Probability Distribution	Divisor	(c_i)	Standard Uncertainty (\pm dB)
Measurement system						
1	Amplitude calibration uncertainty	0.18	N	1	1	0.18
2	Probe anisotropy	0.40	R	$\sqrt{3}$	1	0.35
3	Probe dynamic linearity	0.20	R	$\sqrt{3}$	1	0.12
4	Probe frequency domain response	0.30	R	$\sqrt{3}$	1	0.17
5	Probe frequency linear interpolation fit	0.15	R	$\sqrt{3}$	1	0.09
6	Spatial averaging	0.10	R	$\sqrt{3}$	1	0.06
7	Parasitic E-field sensitivity	0.10	R	$\sqrt{3}$	1	0.06
8	Detection limit	0.0	R	$\sqrt{3}$	1	0.0
9	Readout electronics	0	N	1	1	0
10	Probe positioning	0.19	N	1	1	0.19
11	Repeatability	0.10	N	1	1	0.10
12	Surface field reconstruction	0.20	N	1	1	0.20
Numerical simulations						
13	Grid resolution	0.02	R	$\sqrt{3}$	1	0.01
14	Tissue parameters	0	R	$\sqrt{3}$	1	0
15	Exposure position	0	R	$\sqrt{3}$	1	0
16	Source representation	0.09	N	1	1	0.09
17	Convergence and power budget	0	R	$\sqrt{3}$	1	0
18	Boundary conditions	0.10	R	$\sqrt{3}$	1	0.06
19	Phantom loading/backscattering	0.10	R	$\sqrt{3}$	1	0.06
Combined uncertainty ($k = 1$)						0.49
Expanded uncertainty ($k = 2$)						0.99 (25.6%)

Table 1.2: System check uncertainty budget for psSAR1g measured with DASY8/6 Module WPT V2.8+, assessed according to IEC/IEEE 63184.

System Check Uncertainty Budget for psSAR10g according to IEC/IEEE 63184						
Item	Error Description	Uncertainty Value (±dB)	Probability Distribution	Divisor	(c_i)	Standard Uncertainty (±dB)
Measurement system						
1	Amplitude calibration uncertainty	0.18	N	1	1	0.18
2	Probe anisotropy	0.40	R	$\sqrt{3}$	1	0.23
3	Probe dynamic linearity	0.20	R	$\sqrt{3}$	1	0.12
4	Probe frequency domain response	0.30	R	$\sqrt{3}$	1	0.17
5	Probe frequency linear interpolation fit	0.15	R	$\sqrt{3}$	1	0.09
6	Spatial averaging	0.10	R	$\sqrt{3}$	1	0.06
7	Parasitic E-field sensitivity	0.10	R	$\sqrt{3}$	1	0.06
8	Detection limit	0.0	R	$\sqrt{3}$	1	0.09
9	Readout electronics	0	N	1	1	0
10	Probe positioning	0.19	N	1	1	0.19
11	Repeatability	0.10	N	1	1	0.10
12	Surface field reconstruction	0.20	N	1	1	0.20
Numerical simulations						
13	Grid resolution	0	R	$\sqrt{3}$	1	0
14	Tissue parameters	0	R	$\sqrt{3}$	1	0
15	Exposure position	0	R	$\sqrt{3}$	1	0
16	Source representation	0.04	N	1	1	0.04
17	Convergence and power budget	0	R	$\sqrt{3}$	1	0
18	Boundary conditions	0.10	R	$\sqrt{3}$	1	0.06
19	Phantom loading/backscattering	0.10	R	$\sqrt{3}$	1	0.06
Combined uncertainty ($k = 1$)						0.48
Expanded uncertainty ($k = 2$)						0.97 (25.2%)

Table 1.3: System check uncertainty budget for psSAR10g measured with DASY8/6 Module WPT V2.8+, assessed according to IEC/IEEE 63184.

3.5 Validation

DASY8/6 Module WPT V2.8+ has been validated according to Annex C of IEC/IEEE 63184 [4]. The validation requires determination of psSAR_{1g/10g} (normalized to 1 A (rms) source current) for a set of validation sources and comparison of the peak values to the numerical target values. The results for the validation sources V-Coil350/85 and V-Coil50/400 are summarized in Tables 1.4 and 1.5, respectively.

V-Coil350/85	Measurement [mW/kg]		Target [mW/kg]		Δ [%]	
	1 g	10 g	1 g	10 g	1 g	10 g
Source 1	9.43	7.01	9.49	6.89	-0.6	1.8
Source 2	9.83	7.29	9.49	6.89	3.6	5.8
Source 3	9.89	7.31	9.49	6.89	4.2	6.1

Table 1.4: Summary of measurements performed with three validation sources of the type V-Coil350/85 at 0 mm distance, i.e., the bottom surface of the phantom shell touches the top surface of the source). The uncertainty in the target values is 7.6% ($k = 2$). All values are normalized to 1 A/m (rms) source current. The maximum deviation of 6.1% is well within the combined uncertainty of the target values and the measurement uncertainty of 27%.

V-Coil50/400	Measurement [mW/kg]		Target [mW/kg]		Δ [%]	
	1 g	10 g	1 g	10 g	1 g	10 g
Source 1	13.8	6.92	14.1	6.79	-1.9	1.9
Source 2	13.4	6.68	14.1	6.79	-5.2	-1.6
Source 3	13.3	6.63	14.1	6.79	-5.5	-2.4

Table 1.5: Summary of measurements performed with three validation sources of the type V-Coil50/400 at 0 mm distance, i.e., the bottom surface of the phantom shell touches the top surface of the source. The uncertainty in the target values is 7.6% ($k = 2$). All values are normalized to 1 A/m (rms) source current. The maximum deviation of 5.5% is well within the combined uncertainty of target values and the measurement uncertainty of 27%.

4 Part 2: Evaluation of Compliance with the MPE Limits from 3 – 100 kHz

4.1 System Requirements

To determine the peak incident fields for compliance testing based on MPE as required by §1.1310 of the FCC rules [1] at frequencies < 100 kHz, the following instrumentation is required:

- DASY8/6 Module WPT V2.8+ including:
 - MAGPy-8H3D+E3D Version 2 or Version 3 probe with the integrated data acquisition system MAGPy-DAS
 - MAGPy-RAϕV2 reference probe as a phase reference
 - MAGPy-ES emergency stop system
- WPT sources V-Coil500/3 and V-Coil350/85 for system check and validation purposes
- Software DASY8/6 Module WPT V2.8+

4.2 System Performance Check

Execution of the system performance check before the incident field evaluation of the DUT is recommended. The performance check is equivalent to an assessment of an unknown source for which the target values are known. System performance check with the source V-Coil500/3 or V-Coil350/85 is considered successful if the difference between the H-field measurement result and the target value is smaller than 1.06 dB (13%).

4.3 Assessment of Peak Incident Fields

The workflow to demonstrate compliance of WPT devices with MPE when operating in the frequency range from 3 kHz to 100 kHz is described below and shown in Figure 1.2. More information about each step can be found in Section 7 of the system manual [2].

4.3.1 Volume Scan

In the volume scan, all three components of the H-field (i.e., H_x , H_y , and H_z) generated by the DUT are measured in a volume on top of and as close as physically possible to the DUT. The volume consists of measurement points distributed at uniform steps of 7.33 mm. The scan volume is large enough to include the entire incident field, i.e., the uncertainty with respect to the induced SAR inside the infinite half-space phantom can be assumed to be less than < 0.1 dB.

The peak frequency of the DUT is determined from the spectrum derived by application of FFT to the time-domain signal captured at the reference probe positioned next to the DUT. Zero padding and quadratic fit are applied to improve the resolution of the peak frequency determination. The amplitudes of H_x , H_y , and H_z at the peak frequency are determined by application of DFT to the time-domain signals captured at the corresponding H-field sensors. The phases of H_x , H_y , and H_z (with respect to the reference probe) at the peak frequency are retrieved from the complex-valued frequency-domain data.

With the E-field sensors integrated in the MAGPy probe, amplitudes of all three components of the incident E-field (i.e., E_x , E_y , and E_z) are also measured in the volume scan.

4.3.2 Method of Extra- and Interpolation

The extra- and interpolation operations are both applied to the incident H-field. The surface field reconstruction [2] is achieved by reconstruction based on the curl- and divergence-free conditions of Maxwell's equations. The measured H-fields at upper planes of the scan volume and the reconstructed H-fields at the bottom plane generally correspond to the measurement grid with a uniform step of 7.33 mm; these are tri-linearly interpolated to a fine grid with an approximately uniform step of 1 mm.

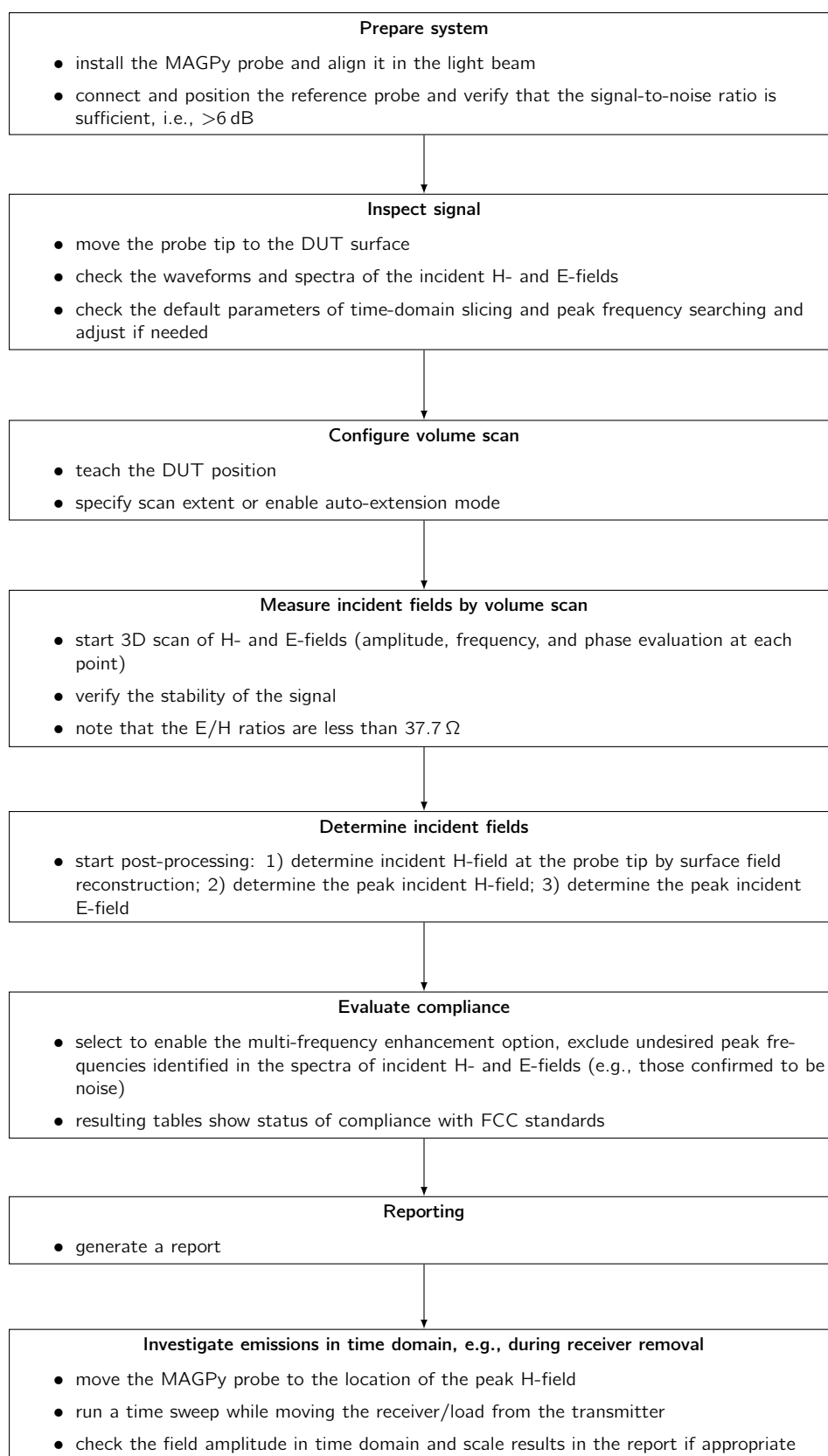


Figure 1.2: Measurement procedure for using DASY8/6 Module WPT V2.8+ to evaluate compliance WPT devices with MPE at frequencies <100 kHz.

4.3.3 Evaluation of Compliance

In the "Compliance (Field values)" table of the DASY8/6 Module WPT V2.8+ manual, the peak values of different field quantities according to the relevant safety standards or regulations are listed; this table facilitates the comparison of the results with the safety limits. In the "Compliance (Ratios)" table, the exposure ratios – i.e., the ratios between the peak field values and the corresponding limits – are listed. This table also provides advanced evaluation options, i.e., total field evaluation, including any exposure due to the incident E-field, and multi-frequency evaluation equivalent to a total-exposure-ratio calculation so that exposures at non-negligible secondary peak frequencies are covered.

4.3.4 Reporting

The report delivered by DASY8/6 Module WPT V2.8+ provides information about the DUT, the software and the probe used in the measurement, the volume scan configuration, visualization of the H-field spectrum and the incident H- and E-field distributions, as well as tables summarizing the peak field values and the exposure ratios for relevant safety standards or regulations.

4.3.5 Time-Domain Evaluation

The highest exposure from a WPT transmitter (e.g., a wireless charger) may take place during the removal of the receiver (e.g., a phone being charged). The time sweep (i.e., zero span) function of DASY8/6 Module WPT V2.8+ enables measurement of the H-field amplitude as a function of time and can be used to investigate the field variation during removal of the receiver. The evaluation results can be scaled according to the field increase observed.

4.4 System Check Uncertainty

The uncertainty in the system check for H-field assessments performed with DASY8/6 Module WPT V2.8+ was determined according to IEC/IEEE 63184 [4] and was documented in the system manual [2], whereby the uncertainty in the calibration is reduced to the repeatability uncertainty, and the isotropic uncertainty is reduced due to the well-defined orientation of the probe to the coil. The detection limit uncertainty is set to zero due to the high signal-to-noise ratio of the source.

4.5 Validation

DASY8/6 Module WPT V2.8+ has been validated according to Annex C of IEC/IEEE 63184 [4]. The validation requires determination of the peak incident H-field (normalized to 1 A (rms) source current) for a set of validation sources and comparison of the peak values to the numerical target values. The validation results for the validation sources V-Coil500/3 and V-Coil350/85 are summarized in Tables 1.8 and 1.9, respectively.

5 Additional Information

Additional information provided in response to the FCC's questions and comments about KDB Inquiry 959118 are attached in the appendices of this document.

6 Conclusions

In this PIA inquiry document, we describe the system requirements, system performance check, measurement procedures, system validation, and uncertainty budget for application of DASY8/6 Module WPT V2.8+ to the testing of compliance of WPT devices with SAR limits (from 100 kHz to 4 MHz) or MPE limits (from 3 kHz to 100 kHz). We also describe methods of the H-field extrapolation/interpolation and the induced field determination.

All steps in the measurement procedures have been optimized and validated. Users cannot interact with or modify any parameter involved in the H-field extrapolation/interpolation and the induced field determination. The

System Check Uncertainty Budget for Peak Incident H-Field according to IEC/IEEE 63184						
Item	Error Description	Uncertainty Value (\pm dB)	Probability Distribution	Divisor	(c_1)	Standard Uncertainty (\pm dB)
Measurement system						
1	Amplitude calibration uncertainty	0.18	N	1	1	0.18
2	Probe anisotropy	0.40	R	$\sqrt{3}$	1	0.23
3	Probe dynamic linearity	0.20	R	$\sqrt{3}$	1	0.12
4	Probe frequency domain response	0.30	R	$\sqrt{3}$	1	0.17
5	Probe frequency linear interpolation fit	0.15	R	$\sqrt{3}$	1	0.09
6	Spatial averaging	0.10	R	$\sqrt{3}$	1	0.06
7	Parasitic E-field sensitivity	0.10	R	$\sqrt{3}$	1	0.06
8	Detection limit	0.0	R	$\sqrt{3}$	1	0.0
9	Readout electronics	0	N	1	1	0
10	Probe positioning	0.19	N	1	1	0.19
11	Repeatability	0.10	N	1	1	0.10
12	Surface field reconstruction	0.30	N	1	1	0.30
Combined uncertainty ($k = 1$)						0.53
Expanded uncertainty ($k = 2$)						1.06 (13.0%)

Table 1.6: System check uncertainty budget for peak incident H-field measured with DASY8/6 Module WPT V2.8+, assessed according to IEC/IEEE 63184.

System Check Uncertainty Budget for Peak Incident E-Field according to IEC/IEEE 63184						
Item	Error Description	Uncertainty Value (\pm dB)	Probability Distribution	Divisor	(c_1)	Standard Uncertainty (\pm dB)
Measurement system						
1	Amplitude calibration uncertainty	0.28	N	1	1	0.28
2	Probe anisotropy	0.60	R	$\sqrt{3}$	1	0.34
3	Probe dynamic linearity	1.00	R	$\sqrt{3}$	1	0.58
4	Probe frequency domain response	0.30	R	$\sqrt{3}$	1	0.17
5	Probe frequency linear interpolation fit	0.15	R	$\sqrt{3}$	1	0.09
6	Parasitic H-field sensitivity	0.20	R	$\sqrt{3}$	1	0.12
7	Detection limit	0.0	R	$\sqrt{3}$	1	0.0
8	Readout electronics	0	N	1	1	0
9	Repeatability	0.10	N	1	1	0.10
Combined uncertainty ($k = 1$)						0.62
Expanded uncertainty ($k = 2$)						1.25 (15.5%)

Table 1.7: System check uncertainty budget for peak incident E-field measured with DASY8/6 Module WPT V2.8+ with linear gradients across the probe, assessed according to IEC/IEEE 63184.

only input available to users is the measured field data. In view of this, we believe the evaluation of the incident fields and psSAR1g/10g down to the DUT surface by DASY8/6 Module WPT V2.8+ should be exempted from NUMSIM PAG.

V-Coil500/3	Measurement [A/m (rms)]	Target [A/m (rms)]	Δ [%]
Source 1	185	179	3.1
Source 2	186	179	3.7
Source 3	188	179	4.9

Table 1.8: Summary of validation measurements performed with three validation sources of the type V-Coil500/3 at 0 mm distance (i.e., the bottom surface of the phantom shell touches the top surface of the source). The uncertainty of the target values are 4.1% ($k = 2$). All values are normalized to 1 A/m (rms) source current. The maximum deviation of 4.9% is well within the combined uncertainty of target value and the measurement uncertainty of 13.6%.


V-Coil500/3	Measurement [A/m (rms)]	Target [A/m (rms)]	Δ [%]
Source 1	243	266	−8.6
Source 2	239	266	−10
Source 3	239	266	−10

Table 1.9: Summary of validation measurements performed with three validation sources of the type V-Coil350/85 at 0 mm distance (i.e., the bottom surface of the phantom shell touches the top surface of the source). The uncertainty of the target values are 4.1% ($k = 2$). All values are normalized to 1 A/m (rms) source current. The maximum deviation of 10% is well within the combined uncertainty of target value and the measurement uncertainty of 13.6%.

Bibliography

- [1] United States Code of Federal Regulations (CFR), Title 47, Section 1.1310, *Radiofrequency radiation exposure limits*, <https://www.ecfr.gov/current/title-47/chapter-I/subchapter-A/part-1/subpart-I/section-1.1310> (Accessed: 6-May-2025).
- [2] SPEAG, *DASY8/6 Module WPT system handbook, incl. SW module WPT 2.8*, December 2024.
- [3] Ilkka Laakso, et al., *Modelling of induced electric fields based on incompletely known magnetic fields*, Phys. Med. Biol., 62, 6567-6587, 2017.
- [4] IEC/IEEE 63184, *Assessment methods of the human exposure to electric and magnetic fields from wireless power transfer systems – Models, instrumentation, measurement and computational methods and procedures (frequency range of 3 kHz to 30 MHz)*, February 2025.

**A Response to FCC's Questions/Comments about KDB Inquiry 959118
(Apr. 3, 2024)**

	Project DASY8/6	Document Name Response for KDB Inquiry 959118	Rev. 2.0
---	-------------------------------	---	------------------------

Response to FCC's Questions/Comments about KDB Inquiry 959118

	Name	Function	Date	Signature
Author	Jingtian Xi	Project Leader, IT'IS		
Approval	Niels Kuster	Quality Manager, IT'IS		

Response to FCC's Questions/Comments about KDB Inquiry 959118

conducted by

Jingtian Xi, Sven Kühn

Zurich, April 3, 2024

The names of IT^{IS} and any of the researchers involved may be mentioned only in connection with statements or results from this report. The mention of names to third parties other than certification bodies may be done so only after written approval from Prof. Dr. N. Kuster.

Revision History

Revisions

- The first report V1.0 responded to the questions/comments received on March 11.
- Revision V2.0 also responds to the additional questions/comments received on March 25.

1 Objective

This report provides the additional information requested in response to the FCC's questions/comments that were received on March 11, 2024 about KDB inquiry 959118. Additional questions/comments were also added to the same inquiry on March 25, 2024. The responses have been compiled by SPEAG's MAGPy team with support from Niels Kuster, Myles Capstick, and Stefan Benkler of the IT'IS Foundation.

2 Detailed Response to Question 1

2.1 FCC's Question/Comment 1

In Section 2.2 (Compliance Testing Requirements), page 2, the issue of the validation is discussed in relation to the 30% agreement requirement of KDB Pub. 680106. To this regard, the statement "As described in Section 6 of the DASY8/6 Module WPT Manual [3], the uncertainty of the surface field reconstruction of DASY8/6 Module WPT V2.4+ is well below this 30% requirement." points to the Reference [3] "SPEAG, DASY8/6 Module WPT system handbook, incl. SW module WPT 2.4, February 2024" that does not seem to be available.

We would like to access at least the relevant section to gain a better understanding of the validation process, in particular referring to the issue of the estimate of the field at touchpoint (the tip of the probe). One would assume that this value is estimated based on the actual field measured in the center of the probe head (or wherever the calibration point is) and on the field gradient, also measured by the probe.

We would like to see details on the validation when this estimate is conducted for the point where the actual field was measured exactly, that is where the probe center can actually be placed (as discussed in the mentioned KDB Pub.).

While we expect that this measurement will work quite well for coils that provide a relatively uniform field along the axis over a characteristic length in the order of the radius of the probe, it would be interesting to see what could be a more challenging case for smaller coils, where the field lines are expected to exhibit a more pronounced to turn off-axis, even at the small distance of the probe radius.

In other words, let's consider r the radius of the probe, R the radius of the coil located in $z=0$ with z being the direction of the coil axis; one can measure the field exactly by placing the center of the probe at $z=r$, and extrapolate the field at $z=0$ (contact position with the coil plane). If $R \gg r$, then the field lines will be relatively "straight" at $z=r$. But if $R \approx r$, the curvature of the field lines will be more pronounced, and one would expect a lesser accuracy of the field estimate at $z=0$.

2.2 SPEAG's Response to Question/Comment 1

2.2.1 Field Reconstruction by Module WPT

DASY8/6 Module WPT V2.4 measures the three orthogonal magnetic (H-) field components, including the phase, on a 7.33 mm grid equivalent to an infinite half-space above the device under test (DUT). The system

continues the H-field measurement until the H-fields at the boundaries are more than 20 dB lower than the maximum field measured. The H-field sensor area is 1 cm^2 , meeting the sensor size requirement as defined in the latest draft of IEC 63184 [1]. The H-field measurement uncertainty at each measurement point is 1.2 dB ($k = 2$, see Section 6.2 of the Module WPT manual [3]).

In the second step, the H-field down to the probe tip (plus the clearance between the probe tip and the DUT surface) is reconstructed with the Maxwell constraint that \vec{H} must remain curl- and divergence-free ($\nabla \times \vec{H} = 0$ and $\nabla \cdot \vec{H} = 0$) to avoid compromising the magnetic vector potential reconstruction. The H-field reconstruction is a Maxwell solution to the vector H-field at the DUT surface that takes the 3D field distribution into consideration and is, therefore, far more accurate than the commonly applied extrapolation of the total H-field.

This surface H-field reconstruction has been validated as documented in Appendix A. The assessed uncertainty is 0.6 dB ($k = 2$), and the full uncertainty budget is provided in Section 6.2 of the Module WPT manual [3].

2.2.2 Field Extrapolation as Determined by MAGPy vs. Other Instrumentation

Section 3.3 of KDB 680106 [4] describes a validation procedure for assessment with standard probes of the uncertainty of the extrapolation to the probe tip. The FCC team expects the uncertainty may increase dramatically if the probe is not much smaller than the diameter of the DUT coil and large compared to the distance to the coil that generates the H-field.

MAGPy V2.4 measures simultaneously the H-fields at eight isotropic sensors. Each of the 8×3 sensors has a loop area of 1 cm^2 , and the centers of the bottom (i.e., closest to probe tip) sensors are 7.5 mm from the surface of the probe tip. A seven-order extrapolation method optimized on the basis of a wide range of simulated configurations (in terms of coil geometry and measurement location) is adopted, which limits the maximum underestimation to 1.6 dB.

When larger sensors are employed, the uncertainty does indeed increase and may exceed 10 dB (see Appendix B). Thus, findings are consistent with the expectations of the FCC team.

2.2.3 Comparison of Surface Field Reconstruction of Module WPT According to the Validation Concept of KDB 680106

Section 3.3 of KDB 680106 [4] describes a validation procedure for standard probes. We tested DASY8/6 Module WPT V2.4 according to this procedure with four system check sources as described in Table 1. The validation measurements consist of four volume scans for each source:

- scan 1: the lowest measurement plane was set to 8.5 mm (the default and the minimum value in DASY8/6 Module WPT V2.4); the spatial peak value of the incident H-field directly measured at 8.5 mm (i.e., without surface field reconstruction) was reported
- scan 2: the lowest measurement plane was set to 17 mm; the spatial peak value of the incident H-field reconstructed at 8.5 mm was reported and compared with the result from scan 1
- scan 3: the lowest measurement plane was set to 28.5 mm; the spatial peak value of the incident H-field directly measured at 28.5 mm (i.e., without surface field reconstruction) was reported
- scan 4: the lowest measurement plane was set to 37 mm; the spatial peak value of the incident H-field reconstructed at 28.5 mm was reported and compared with the result from scan 3

The scan volume sizes are large enough to cover the spatial peak of the H-field. The measured and reconstructed H-fields and the deviations between them are provided in Table 2. The maximum deviation between the actual measurement and the reconstruction measurement is less than 23%, i.e., the surface field reconstruction based on volume scan data is accurate not only on large sources (i.e., $R \gg r$, e.g., sources 1 and 2) but also on small sources (i.e., $R \approx r$ or even $R < r$, e.g., sources 3 and 4).

Source no.	Frequency [kHz]	Outer diameter [mm]	Inner diameter [mm]	No. of turns
1	3	454	227	11
2	85	350, 200	314, 164	13
3	400	50	22	8
4	6,780	30.75	10.75	10

Table 1: Operation frequencies, dimensions, and numbers of turns for the four system check sources used in the validation measurements

Source no.	Distance d [mm]	$H_{\text{tot,max},d}$ measured [A/m, rms]	$H_{\text{tot,max},d}$ reconstructed from $d + 8.5$ mm [A/m, rms]	Deviation [%]
1	8.5	109	104	-4.6
1	28.5	52.3	52.5	0.4
2	8.5	132	120	-9.1
2	28.5	57.5	58.3	1.4
3	8.5	138	129	-6.5
3	28.5	27.8	27.4	-1.4
4	8.5	80.5	62.2	-22.7
4	28.5	9.93	8.82	-11.2

Table 2: Results of the measured H-fields and H-fields reconstructed from measurements made with DASY8/6 Module WPT V2.4 with the bottom sensors placed at a distance $d + 8.5$ mm above the four system check sources.

3 Detailed Response to Question 2

3.1 FCC's Question/Comment 2

The second item is related to the SAR estimate provided for $f < 4$ MHz. In this case we understand (e.g., Section 3.2) that sampling of the incident field, followed by a field reconstruction. In this Section, it is mentioned that: "The SAR induced by the incident E-field is determined by a conservative approximation that is valid for local E-field sources [6]." Is the reference [6] sufficient for gathering the details of this approach?

The uncertainty of this process is discussed in Section 4.3, that reads: "The uncertainty for evaluations performed with DASY8/6 Module SAR 16.2+ was determined according to IEC/IEEE 62209-1528:2020 [8] and documented in the DASY8/6 Module SAR 16.2+ Manual [7]." We would like to review mentioned the discussion in [7], either excerpt of the manual or other reference papers would be fine.

... we added additional information to KDB 959118, more specifically focused on the issue of using the probe SAR estimates for compliance purposes.

3.2 SPEAG's Response to Question/Comment 2

3.2.1 SAR Assessment with DASY8/6 Module SAR V16.2

DASY8/6 Module SAR V16.2 directly measures the induced SAR in the specified phantom without any approximation or simulation. Therefore, it is valid for any source. At present, the lower limit of the frequency measured with SPEAG's dosimetric probes is 4 MHz. Dosimetric probes for lower frequencies are currently under development. Hence, DASY8/6 Module SAR V16.2 is recommended for SAR assessment at frequencies greater than 4 MHz as DASY8/6 Module SAR V16.2 is the most accurate system. Section 4.3 of the application note [5] provides the uncertainty of SAR measurements made with DASY8/6 Module SAR V16.2. Details of the uncertainty evaluation are documented in Section 6 of the Module SAR manual [7]. A copy of the manual will be provided with this response.

3.2.2 SAR Assessment with DASY8/6 Module WPT V2.4

DASY8/6 Module WPT V2.4 is suitable for SAR assessments at frequencies below 4 MHz (and incident field assessments at frequencies below 10 MHz). Section 3.2 of the application note [5] summarizes the key technologies implemented in DASY8/6 Module WPT V2.4.

In DASY8/6 Module WPT V2.4, the following three steps are used to determine the psSAR1g:

- Step 1a: The incident H-field including the phase is scanned in the half-space including the exposed phantom.
- Step 1b: During the same scan, the incident electric (E-) field is measured and evaluated, and it is determined whether the incident E-field is caused by a local charge accumulation and whether the overall field impedance is much less than 377Ω . If this is the case, it can be tested by applying concepts in [6] to demonstrate whether the psSAR1g induced by the incident E-field is negligible compared to that induced

by the incident H-field. If this can be shown, the incident E-field does not need to be considered for demonstration of compliance¹.

- Step 2: The H-field down to the probe tip (plus the clearance between the probe tip and the DUT surface) is reconstructed with the Maxwell constraint that \vec{H} must remain curl- and divergence-free ($\nabla \times \vec{H} = 0$ and $\nabla \cdot \vec{H} = 0$) to avoid compromising the magnetic vector potential reconstruction afterward.
- Step 3: The E-fields induced in the phantom by the reconstructed and measured H-field are simulated, and the standardized averaging method is used to determine the maximum psSAR1g. The total uncertainty of psSAR1g is provided in the application note.

¹The reference levels for E-field exposure at low frequencies have been determined by applying a constant E-field between head and feet of the human body, i.e., the human is between two conductors of a capacitor, which results in maximum induction of currents.

4 Detailed Response to Question 3

4.1 FCC's Question/Comment 3 (received on March 25, 2024)

This is in reference to the Appendix B “Effect of Backscattering” that addressed our question about the estimating the near field based on the source (coil) measurements without phantom, that in this case provides the typical load. Our question was motivated by the need of quantifying the impact of the presence of the load on the field estimate that then leads to the calculation of SAR. This is important because we want to make sure that the proposed method for estimating SAR is general enough to be accepted in our compliance guideline.

The Appendix B discusses the conditions under which the induced (eddy) current in the phantom does not alter the incident field: in many cases that is a good approximation, although there are cases where that is not the case.

However, we would like to point out that neglecting the flux cancellation due to the induced current in the phantom always leads to a conservative estimate for the purpose of computing SAR. This appears to be a key point for the MAGPy technology under consideration, and does support the “conservative” estimate for SAR as mentioned when referring to [6]; however the approach we mentioned does not seem to be have been not discussed in your write-up, unless we missed it,

In other words, assuming that the induced current does not reduce (significantly) the incident field leads to estimating a larger induced E-field (i.e., the field that supports the eddy current) in the phantom. This electric field is what determines SAR, thus SAR will be overestimated (a conservative result) if the mentioned assumption is not accurate.

Please let us know if this analysis is indeed along the lines of what you intended to present. Any further development in this direction twill provide an avenue for a faster consideration of taking advantage of the MAGPy approach for our compliance testing.

Some details follow, to clarify the statements just made. In the Appendix B, the case where the effect of the phantom load can be neglected was quantified in the equations (6):

$$\omega^2 \epsilon \mu L^2 \ll 1 \quad (6a)$$

$$\omega \sigma \mu L^2 \ll 1 \quad (6b)$$

Since $c = 1/\sqrt{\epsilon\mu}$, eq. (6a) can be re-written as $L \ll \lambda/(2\pi)$, that is the usual criterion of specifying the reactive near field distance, and where the quasi-static approximations hold. Similarly, (6b) can be re-written as $L \ll 1/\sqrt{\omega\sigma\mu}$, i.e. L needs to be much smaller than the skin depth, besides a factor $1/\sqrt{2}$.

In the document, the length L in equation (6) is referred to the coil diameter. However, the length L referred to the phantom/load typical thickness would lead to a more general applicability. The reason for this is that the thickness of the phantom (i.e., the conductor where the currents are induced) is the key parameter to determine if the induced currents are sufficient to affect the incident field via flux cancellation.

It can be shown that when the skin depth is much larger than the applicable thickness of the device, then the flux cancellation due to the induced current is negligible as compared to the incident flux. In other words, the

induced current can be computed solely based on the incident magnetic field. This is a known result from eddy current analysis, and corresponds to what is referred to as resistance-limited (as opposed to reactance-limited) case.

In this case, the imposed magnetic field is essentially unaffected by the reaction of the eddy currents (however, those currents can still provide a meaningful energy dissipation).

Any further comments on these matters will be useful.

4.2 SPEAG's Response to Question/Comment 3

Thank you very much for your constructive feedback and we agree with the statements above:

- *Equations (6a) and (6b) with wave length and skin depth:* The document has been extended to take over these simplifications (equation (7) and (8) in the attached revised and amended document).
- *neglecting the flux cancellation due to the induced current in the phantom leads to a conservative estimate:* we agree but would add that the overestimation is small. We also added this point to application note.
- *In the document, the length L in equation (6) is referred to the coil diameter. However, the length L referred to the phantom/load typical thickness would lead to a more general applicability. The reason for this is that the thickness of the phantom (i.e., the conductor where the currents are induced) is the key parameter to determine if the induced currents are sufficient to affect the incident field via flux cancellation.* We improved the definition of the criteria and expressed in terms of skin-depth. For practical systems operating below 4 MHz this criteria is generally fulfilled.

5 Conclusions

With DASY8/6 Module WPT V2.4, the surface field reconstruction is adopted to determine the incident H-field down to the DUT surface. The field reconstruction is more advanced and more accurate than any field extrapolation based on curve fitting. The preliminary uncertainty of 0.6 dB ($k = 2$) has been assessed by statistical means.

With DASY8/6 Module WPT V2.4, the incident H- and E-fields are determined, and simulations are used to estimate the psSAR1g directly from the measured and reconstructed H-fields. Neglecting the flux cancellation due to the induced current in the phantom leads to a small overestimation and therefore is not considered in the uncertainty estimation. DASY8/6 Module WPT V2.4 automatically verifies that the psSAR1g induced by the incident E-field can be neglected, as is always the case for localized, non-invasive E-field sources.

DASY8/6 Module SAR V16.2 is the most accurate system for determination of the psSAR1g at frequencies greater than 4 MHz, as it is a direct dosimetric measurement system that does not involve application of any field reconstruction or approximation.

References

- [1] IEC 63184, *Assessment Methods of the Human Exposure to Electric and Magnetic Fields from Wireless Power Transfer Systems - Models, Instrumentation, Measurement and Computational Methods and Procedures (Frequency Range of 3 kHz to 30 MHz)*, Committee Draft for Vote (CDV), August, 2023.
- [2] SPEAG, *MAGPy V2.4 Manual*, February, 2024.
- [3] SPEAG, *DASY8 Module WPT System Handbook Including SW Module WPT 2.4*, February, 2024.
- [4] FCC KDB 680106 D01 v04, *Equipment Authorization of Wireless Power Transfer Devices*, October 2023.
- [5] SPEAG, *Testing WPT Devices with DASY8/6 Modules WPT and SAR for Compliance with FCC KDB 447498/680106*, January, 2024.
- [6] A. Christ, A. Fallahi, E. Neufeld, Q. Balzano, and N. Kuster, *Mechanism of Capacitive Coupling of Proximal Electromagnetic Sources With Biological Bodies*, *Bioelectromagnetics*, 43(7), 2022.
- [7] SPEAG, *DASY8 Module SAR System Handbook Including SW Module SAR 16.2*, May, 2023.
- [8] IEC/IEEE 62209-1528, *Measurement Procedure for the Assessment of Specific Absorption Rate of Human Exposure to Radio Frequency Fields from Hand-Held and Body-Worn Wireless Communication Devices (Frequency range of 4 MHz to 10 GHz)*, October, 2020.
- [9] Spectrum Management and Industry Canada Telecommunications, *Radio Standards Specification, SPR-002, Supplementary Procedure for Assessing Compliance of Equipment Operating from 3 kHz to 10 MHz with RSS-102*, Issue 2, 2022.

A Validation of Surface Field Reconstruction

The surface field reconstruction method has been validated for different distances from the coil by comparing the H-field and induced SAR reconstructed on the basis of values simulated on a uniform regular measurement grid to the values determined from simulations. The diameter of the coil geometry is varied from 50 mm to 450 mm, and the filling ratio ranges from 0.1 to 0.9. The detailed assessment workflow is illustrated in Figure 1.

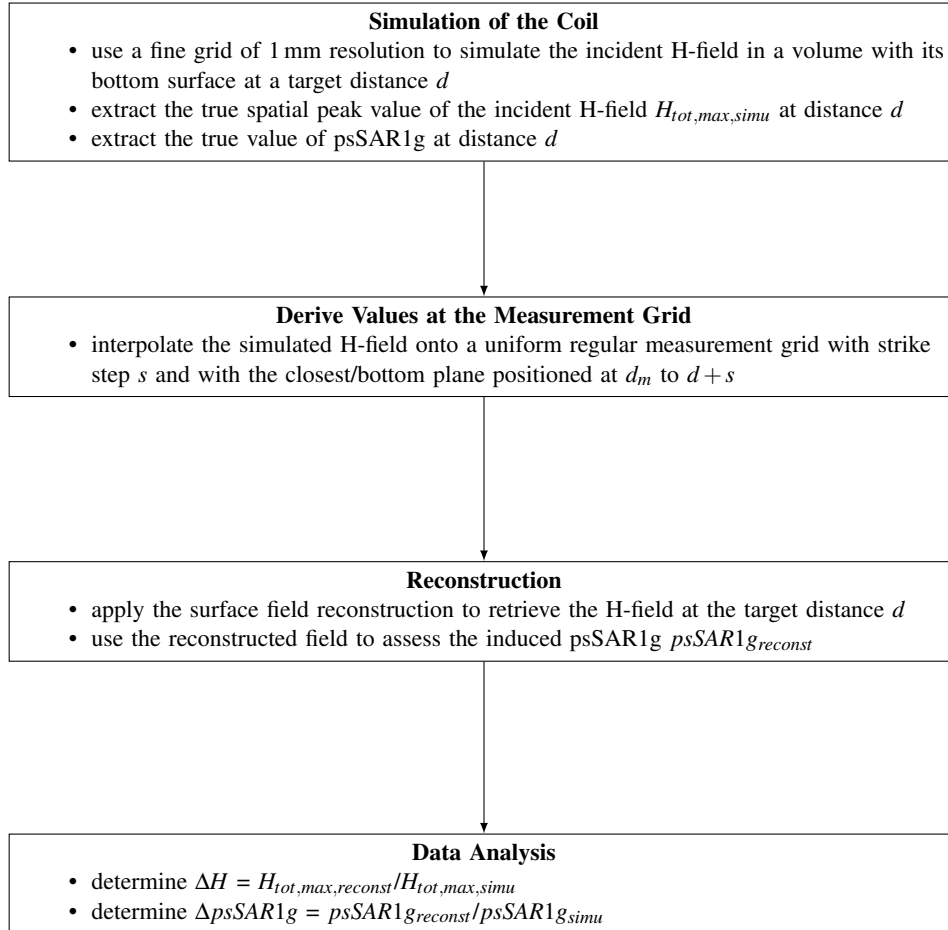


Figure 1: Module WPT procedure for validation and assessment of the uncertainty of the field reconstruction.

The results demonstrate that the maximum difference between the reconstructed fields and their true values decreases as the grid step s becomes finer, especially for very localized sources. For the implemented grid step s of 7.33 mm in DASY8/6 Module WPT V2.4, ΔH ($k = 1$) is less than 0.3 dB and for $\Delta psSAR1g$ ($k = 1$) is less than 0.2 dB.

B Extrapolation of the H-Field without Reconstruction Based on the H-Field Information on a Dense Uniform Regular Grid

The field gradient uncertainty depends on the method applied by the measurement system to evaluate the field gradient. Commonly used larger three-axis probes that integrate the field over loops do not appropriately capture the maximum fields at the smallest possible distance from the DUT. These loops may not be specified for measurements at close distances (see, e.g., Clause 7.1.7.1 of [9]) and can be assumed to be prone to significant uncertainties when fields with high gradients are measured.

Figure 2 shows a probe with three pick-up loops measuring the H-field at distance d above the cover of a WPT system. The deviation of the measured field integrated over the areas of the three loops from the actual H-field maximum at the cover of the WPT system for the 70 different generic WPT coils evaluated in [2] is given in Figure 3 as a function of the probe diameter. The errors of the 70 different cases is normalized to the mean value for their respective radii. The mean values are given as figures in the plots below the respective error distributions. The deviations of a gradient probe, which uses a pick-up loop with 5 mm radius for the measurements of surface fields, are given for comparison [2]. This has already been evaluated in [9]. The required measurement distance of $1.7 \times$ the probe diameter cited in [9] greatly reduces the uncertainty of the measurements but does not allow evaluation of the exposures at smaller distances with reasonable uncertainty.

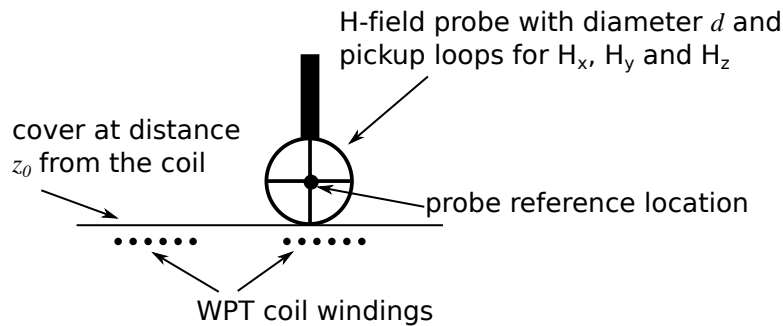


Figure 2: H-field probe with pickup loops of diameter d for the three vector components above the windings of a WPT coil. The probe tip touches the cover of the WPT system and is located at distance z_0 from the coil. The probe reference location is in the probe center at $0.5d + z_0$.

The results shown in Figure 3 demonstrate that the uncertainty of the H-field measured by three-axis probes with large pick-up loops increases as a function of the probe diameter. For a diameter of 100 mm, the uncertainty can exceed 20 dB. The deviations of the gradient probe are within 2 dB for the evaluated coils, as it utilizes small sensors as close as possible to the probe tip. In comparison, the preliminary uncertainty of DASY8/6 Module WPT V2.4 measurements based on the H-field information in the entire volume for the field reconstruction is 0.6 dB.

Figure 4 shows the magnitude of the H-field for a subset of the 70 generic WPT coils shown in Figure 3 [2] as a function of the height above the coil at different distances from the center axis, normalized to the value at distances of 20 mm, 40 mm, and 50 mm. For a normalization distance of 20 mm, the maximum fields at the DUT surface are about 35 dB higher than the value at 20 mm. At the larger normalization distances of 40 mm and 50 mm, the maximum fields at the DUT surface are as much as 50 dB greater than the value at the normalization distance. The fields at distances larger than the normalization distance are within the same order of magnitude for 40 mm and 50 mm. In conclusion, it is not possible to predict the slope of the field gradient

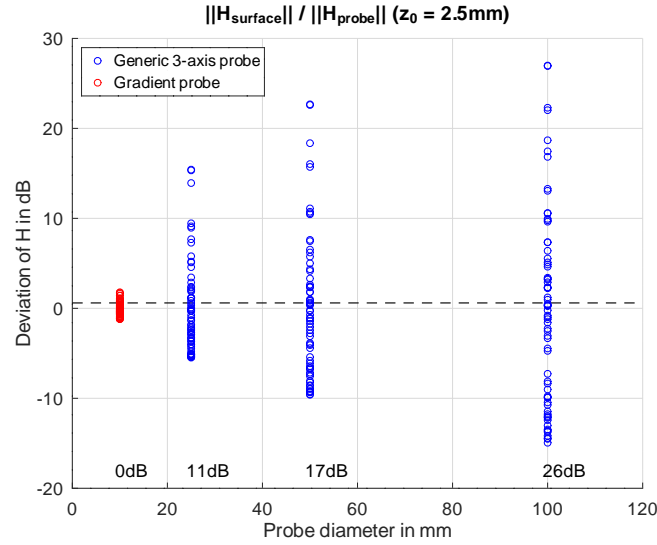


Figure 3: Deviation of the H-field $||H_{\text{surface}}||$ at the surface of the DUT from the readout $||H_{\text{probe}}||$ when determined with probes with diameter d (Figure 2) at $z_0 = 2.5$ mm above 70 different generic WPT coils [2], with the mean decay value used for extrapolation. The uncertainty is 10 dB for a diameter of 25 mm and 20 dB for a diameter of 50 mm. The uncertainty can be reduced to 2 dB only for probe diameters < 10 mm when measured gradient information is used. The dashed line indicates the uncertainty of the surface field reconstruction of DASY8/6 Module WPT V2.4.

from measurements at the larger normalization distances. Extrapolation of the maximum field at positions close to the WPT coil is therefore always prone to uncertainty.

Figure 4 illustrates that, for fields that decay rapidly as a function of distance from the source, the source model cannot be validated at large distances, because the different field configurations are similar at larger distances. This conclusion is made clear by the small spread of the curves at the end of the z -axis in the plot for normalization at 50 mm while having largely different exposure fields at the surface of the DUT, as shown by the large spread at $z = 0$ in the same plot. This uncertainty increases with the distance of the probe from the surface as well as with the probe diameter.

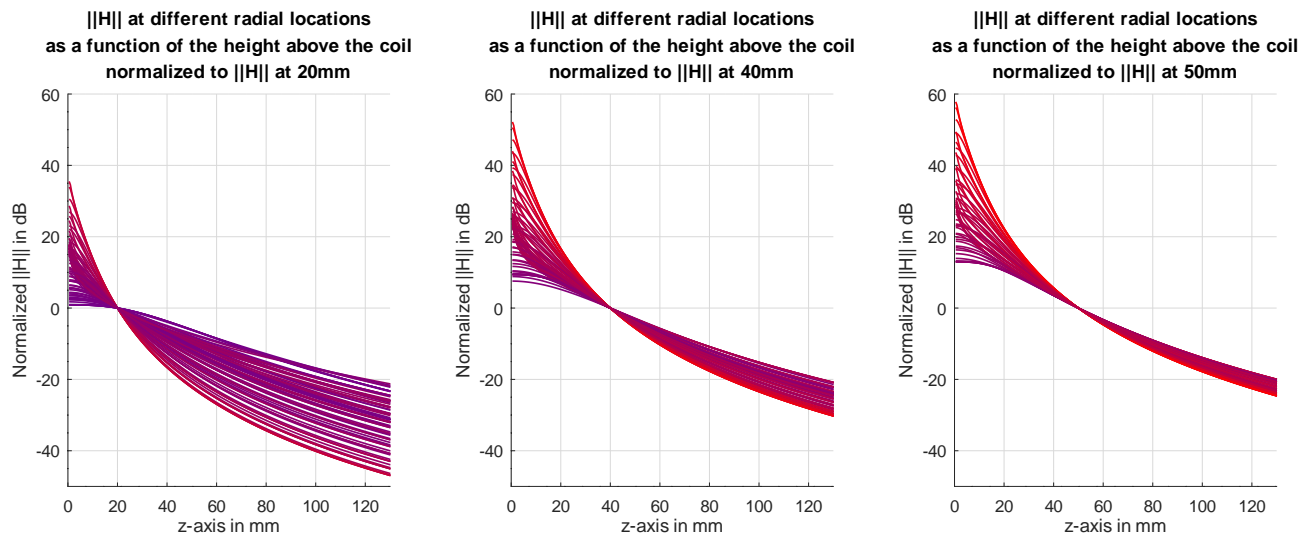



Figure 4: The magnitude of the H-field for a subset of the 70 generic WPT coils shown in Figure 3 [2], as a function of the height along the z -axis above the coil at different distances from the center axis, normalized to the value at distances of 20 mm, 40 mm, and 50 mm.

**B Response to FCC's Questions/Comments about KDB Inquiry 959118
(May 13, 2024)**

	Project DASY8/6	Document Name KDB Inquiry 959118	Rev. 20240422/1.0
---	-------------------------------	--	---------------------------------

**Additional Information Addressing FCC's Response of April 22, 2024
KDB Inquiry 959118**

	Name	Function	Date	Signature
Author	Jingtian Xi	Project Leader, IT'IS		
Approval	Niels Kuster	Quality Manager, IT'IS		

Additional Information Addressing FCC's Response of April 22, 2024 KDB Inquiry 959118

conducted by

Jingtian Xi, Sven Kühn

Zurich, May 13, 2024

The names of IT'IS and any of the researchers involved may be mentioned only in connection with statements or results from this report. The mention of names to third parties other than certification bodies may be done so only after written approval from Prof. Dr. N. Kuster.

1 Objective

This report provides the additional information requested in response to the FCC's questions/comments that were received on April 22, 2024 about KDB inquiry 959118. The responses have been compiled by the IT'IS Foundation and SPEAG's MAGPy team.

2 Additional Information Addressing FCC's Response Dated April 22nd, 2024

2.1 FCC's Question/Comment 1 (FCC's Response of 20240422)

thank you for the additional information in the new document of April 12, 2024. We note that the Table 1 in Page 4/5 shows significant discrepancies among the errors computed with the various approaches. Albeit the MAGPy is clearly performing better, it would be interesting to understand what leads to the large changes between Profile #2 (that yields a small 3.61% error) and the other profiles (errors in the 20% range).

We outlined in the previous reply the validation of the extrapolation method (that is, using the probe without the field reconstruction), and we expanded that in more detail in the latest Apr 2024 TCBC workshop (Presentation 4.2).

We would be interested to see if the MAGPy extrapolation formula (i.e., without field reconstruction) is providing good enough results. Since the MAGPy radius is only 7.5 mm, one would need to: 1) Position the probe with the tip in contact with the DUT, thus measuring the field at 7.5 mm exactly, and extrapolating the field at 0 mm. 2) Move the probe with the tip 7.5 mm from the DUT. Thus, the probe center is now at 15 mm. Use this setup to extrapolate the field at 7.5 mm and compare with the measurement in step 1).

If this validation leads to an error less than 30%, we would accept the extrapolation procedure for the probe for the purpose of compliance, and therefore we would accept the extrapolated field at 0 mm in step 1).

2.2 Additional Information/Clarifications Addressing Question/Comment 1

The decay of the H-field as a function of the distance from the coil greatly depends on the source and location.

Figure 1 shows that if we are able to measure the field accurately at 20 mm, the field at the surface is between 0 dB and 38 dB (1–80 times) of the value at 20 mm. If the field is accurately measured at 7.5 mm, the variation is reduced to 0 dB and 17 dB (1–7 times) of the value at 7.5 mm. In other words, the measurement at 7.5 mm is not sufficient to determine the field at the surface with an uncertainty of $\pm 30\%$ as requested by FCC [1].

MAGPy2 V2.4+ solves the problem with the following approach:

- measure the field accurately at 7.5 mm and 29.5 mm from the surface,
- determine the gradient,
- extrapolate using the function for magnitude and gradient described in Section 2.3.8 of the MAGPy Manual V2.4 [2]. It has been determined by optimizing the uncertainty (of the underestimation) such that it is less than ± 2 dB ($\pm 26\%$, $k = 2$).

We believe that the procedure meets the FCC criteria of $\pm 30\%$. It has been validated using several thousands different realistic H-field decays/profiles.

If we would measure as suggested at 7.5 mm and take another measurement with an offset of 7.5 mm (i.e., at 15 mm from the surface) and use this information to find an optimal extrapolation function to estimate the field at the surface, the results would be more accurate since the gradient would be more accurate. However, the final uncertainty would be prone to user errors and affected by the uncertainty of the 7.5 mm shift.

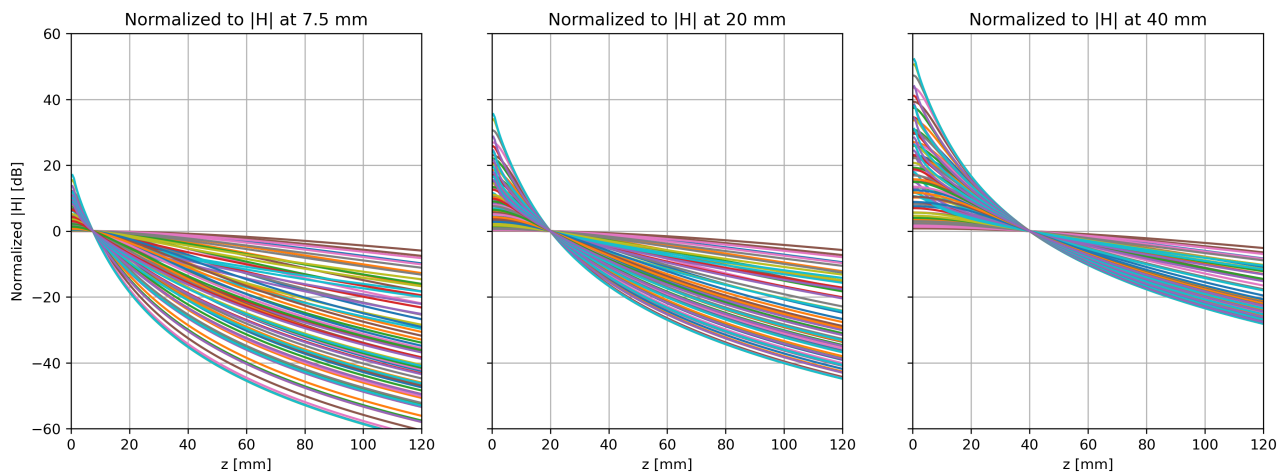


Figure 1: The magnitude of the H-field for a subset of the 70 generic WPT coils [2], as a function of the height along the z -axis above the coil at different distances from the center axis, normalized to the value at distances of 7.5 mm, 20 mm, and 40 mm (same Figure as included in our document of April 3, 2024 [3] but with the information for 7.5 mm)

2.3 FCC's Question/Comment 2

In regard to the question on the NUMSIM PAG, the PAG requirement is there only because of the novelty of the method and the limited validation cases that we could examine so far. The NUMSIM PAG is triggered (in general, not just for the MAGPy+field reconstruction) when the test data are supplemented/augmented by a numerical model.

This would no longer be the case when it has been clarified what the limits of validity of the model are, and we have sufficient evidence that a compliance test lab (even with limited numerical experience) is protected from use cases where the model is not sufficiently accurate. This could be the case previously discussed, where the E/H ratio is too large.

Based on the information we accessed so far, we actually have no reasons to doubt about the correctness of the field reconstruction algorithm per se. The concerns from a compliance perspective stem from the need to ensure that the users are prevented from applying the method incorrectly or, in other words, to gain information about "failsafe scenarios", error messages, self-check procedures, etc. all provided as part of the s/w package.

A draft of the NUMSIM PAG checklist (essentially what the applicant needs to submit/show) was also presented at the April 2020 TCBC workshop. This is not yet in effect, it is just a draft.

We realize that there are folks with limited numerical simulation experience, that may not be able to provide that type of information, but rather rely on the test probe and software manufacturer for the validation aspect. That is why we are considering to focus more on procedures that clearly prevent the incorrect utilization of the methodology, as discussed above.

2.4 Additional Information/Clarifications Addressing Question/Comment 2

2.4.1 SAR Assessment Methodology in DASY8/6 Module WPT V2.4+

The unique feature of DASY8/6 Module WPT V2.4+ is that it measures the 3D distribution of the incident H-field emitted by the DUT including phase. It uses the measured field information to reconstruct the SAR in the standardized phantom. The reconstruction is performed in the following three steps:

- Step 1 (validated algorithm): The H-field down to the probe tip (plus the clearance between the probe tip and the DUT surface) is reconstructed with the Maxwell constraint that \vec{H} must remain curl- and divergence-free ($\nabla \times \vec{H} = 0$ and $\nabla \cdot \vec{H} = 0$) to avoid compromising the magnetic vector potential reconstruction. The H-field reconstruction is a Maxwell solution to the vector H-field at the DUT surface that takes the 3D field distribution into consideration and is, therefore, far more accurate than the commonly applied extrapolation of the total H-field. The assessed uncertainty is 0.6 dB ($k = 2$), and the full uncertainty budget is provided in Section 6.2 of the Module WPT manual [4].
- Step 2 (validated solver [5]): The E-field distribution in the standardized phantom is determined using the Magneto Quasi-Static (MQS) solver of Sim4Life and the measured/reconstructed field information of Step 1.
- Step 3 (validated algorithm): The psSAR1g is determined using the standardized spatial-averaging algorithm [6] and the simulated field distribution of Step 2.

The system is self-contained. The procedure does not require any input by the users of DASY8 Module WPT

other than teaching the compliance plane. The system automatically performs all checks needed to ensure accurate reconstructed psSAR1g values within the specified uncertainty.

In order to exclude any user error or system error, we recommend that the user perform a system verification (applying the same procedure) by evaluating the verification source that is the closest to the DUT with respect to the frequency. If the results are compliant with the verified target values, the system is ready to be applied to the DUT.

2.4.2 Detailed Response to NUMSIM PAG Items

Here we try to provide the information regarding all the items in the check list for the NUMSIM PAG presented at the TCB workshop on April 17, 2024 [7].

1. Show that the simulation model provides a conservative estimate of the actual RF exposure conditions.

Example. The simulation domain is larger than what corresponds to actual conditions based on a known radiation pattern of the DUT for the applicable test separation distance, and the choice of simulated phantom parameters (such as conductivity and dielectric permittivity) is consistent with the use conditions.

The system ensures that the entire emitted field is measured and used to reconstruct the psSAR1g in the standardized phantom at the location taught by the user. The phantom (approximating half-space with 2 mm shell) filled with the tissue simulating liquid ($\sigma = 0.75 \text{ S/m}$, $\epsilon_r = 55$, and $\rho = 1000 \text{ kg/m}^3$) corresponds to that defined by FCC and other standard organizations [8, 9] and cannot be altered by the user. If the criteria of the field extent are not met, the system provides warning information (e.g., boundary effect warning) to the user in its automatically generated report. The system manual also provides guidance to the user about how to best address the field extent problem.

2. Describe how the simulation model is used to show compliance. *Example: modeling a small volume of body tissue that is sufficient to represent the worst-case illumination conditions from the transmitter EM field.*

As explained in item 1, the homogeneous phantom used by DASY8/6 Module WPT V2.4+ is equivalent to a half-space phantom on top of the DUT. Therefore, DASY8/6 Module WPT V2.4+ guarantees that the worst-case illumination conditions are captured.

3. Discuss how the modeling results are leveraged, directly or indirectly, to show compliance. *Example: The EM field is computed to show that the E/H ratio is small enough to consider the transmitter "predominantly magnetic," thus allowing compliance to be shown only based on magnetic field probe measurements.*

In line with KDB 680106 [1], DASY8/6 Module WPT V2.4+ computes the E/H ratio based on the E- and H-fields measured with the MAGPy V2 probe and reports it as one indicator to determine if the DUT is producing a magnetic dominant near field. In addition, DASY8/6 Module WPT V2.4+ has incorporated a method to estimate the SAR induced by the incident E-field [10] and hence enables checking if the exposure due to the incident E-field can be neglected directly.

4. Discuss how the model and its numerical input data have been chosen to provide a realistic simulation.

Example: The EM field is computed to show that the E/H ratio is small enough to consider the transmitter "predominantly magnetic," thus allowing compliance to be shown only based on magnetic field probe measurements.

DASY8/6 Module WPT V2.4+ does not require modeling of the DUT.

5. Demonstrate that the results are converged from the perspective of the choice of key numerical parameters. *Changes in the EM field solution (or applicable derived indicators such as SAR and Power Density) become increasingly small for smaller grid size and time steps.*

DASY8/6 Module WPT V2.4+ uses the validated Magneto Quasi-Static (MQS) solver of Sim4Life to determine psSAR_{1g} up to 4 MHz. Since the MQS solver is a frequency domain solver, it has no time step. It uses a uniform 1 mm resolution across x, y, and z axes and a computation domain surrounding the whole volume scanned. The associated uncertainties for these two numerical parameters are ≤ 0.1 dB ($k = 2$) [4]. As the flux cancellation due to the induced currents are neglected, psSAR_{1g} results are always conservative.

6. Verify the consistency of simulated EM field vs. basic physical requirements. *Example. Continuity of perpendicular and tangential components of the EM field across a material interface, $\text{div } B=0$, etc.*

The Finite Element Method code of the MQS solver used by DASY8/6 Module WPT V2.4+ fulfills all physical boundary conditions by using linear nodal elements for the scalar potential field.

7. Validate the model as applied to the specific DUT simulation. *Example. Compare EM solution vs. measured data and compare with theoretical predictions for applicable configurations. On the other hand, calculations or measurements for quasi-static conditions cannot be used for a full-wave simulation at higher frequencies.*


DASY8/6 Module WPT V2.4+ does not require modeling of the DUT and directly uses the emitted field to reconstruct the psSAR_{1g}.

References

- [1] FCC KDB 680106 D01 v04, *Equipment Authorization of Wireless Power Transfer Devices*, October 2023.
- [2] SPEAG, *MAGPy V2.4 Manual*, February, 2024.
- [3] J. Xi and S. Kühn, *Response to FCC's Questions/Comments about KDB Inquiry 959118*, April 3, 2024.
- [4] SPEAG, *DASY8 Module WPT System Handbook Including SW Module WPT 2.4*, February, 2024.
- [5] G. Tsanidis, T. Samaras, *Verification Report of Sim4Life and SEMCAD X Low Frequency Magnetic Quasi-Static Solver*, July, 2015.
- [6] IEC/IEEE 62704-1, *Determining the peak spatial-average specific absorption rate (SAR) in the human body from wireless communications devices, 30 MHz to 6 GHz - Part 1: General requirements for using the finite difference time-domain (FDTD) method for SAR calculations*, October, 2017.
- [7] Alfonso G. Tarditi, *Part 18 Wireless Power Transfer Devices: Clarifications on KDB 680106v04 and ECR Processes*, April, 2024.
- [8] IEC 63184, *Assessment Methods of the Human Exposure to Electric and Magnetic Fields from Wireless Power Transfer Systems - Models, Instrumentation, Measurement and Computational Methods and Procedures (Frequency Range of 3 kHz to 30 MHz)*, Committee Draft for Vote (CDV), August, 2023.

- [9] ISED SPR-002 Issue 2, *Assessment methods of the human exposure to electric and magnetic fields from wireless power transfer systems – Models, instrumentation, measurement and computational methods and procedures (Frequency range of 3 kHz to 30 MHz)*, October 2022.
- [10] A. Christ, A. Fallahi, E. Neufeld, Q. Balzano, and N. Kuster, *Mechanism of Capacitive Coupling of Proximal Electromagnetic Sources With Biological Bodies*, *Bioelectromagnetics*, 43(7), 2022.

**C Response to FCC's Questions/Comments about KDB Inquiry 959118
(Feb. 15, 2025)**

	Project DASY8/6	Document Name KDB Inquiry 959118	Rev. 1.0
---	-------------------------------	--	------------------------

**Additional Information Addressing FCC's Response
of October 18, 2024 KDB Inquiry 959118**

	Name	Function	Date	Signature
Author	Jingtian Xi	Project Leader, IT'IS		
Approval	Niels Kuster	Quality Manager, IT'IS		

Additional Information Addressing FCC's Response of October 18, 2024 KDB Inquiry 959118

conducted by

Stefan Benkler, Jingtian Xi, Niels Kuster

Zurich, February 15, 2025

The names of IT'IS and any of the researchers involved may be mentioned only in connection with statements or results from this report. The mention of names to third parties other than certification bodies may be done so only after written approval from Prof. Dr. N. Kuster.

1 Objective

This report contains the requested additional information in response to the discussion with FCC on October 18, 2024 about

- determination of the incident H-field at the surface of the probe in DASY8/6 Module WPT V2.6+ using the surface field reconstruction, and
- providing the rationale why the determination of the psSAR1g induced in the standardized flat phantom by DASY8/6 Module WPT V2.6+ should be exempted from the NUMSIM PAG requirement.
- remove the wrong references to Sim4Life from the manual since Sim4Life is not a component of DASY8/6 Module WPT V2.6+. However, the measured file is compatible with Sim4Life so that it can be imported and additional detailed analysis performed using the full functionality of the advanced Sim4Life simulation platform in combination with any of the different ViP models.

The responses have been compiled by the IT'IS Foundation and SPEAG's MAGPy team.

2 Determination of the incident H-field at the surface of the probe in DASY8/6 Module WPT V2.6+ using the surface field reconstruction

IT'IS will provide evidence that the surface field reconstruction of Module WPT does not include any simulations nor parts of sim4life (in this case, it can potentially be exempted from NUMSIM PAG).

The H-field is reconstructed by using the curl- and divergence-free conditions of Maxwell's equations. The curl- and divergence-free nature is essential for the upcoming vector potential reconstruction (base assumption in 3.2). Assuming the magnetic flux density B_{ijk} is known on a rectilinear lattice for any i and j but only for $k \geq 1$, that is, $k = 0$ needs to be extrapolated:

1. B_{ij0}^x : Using the y-component of $\nabla \times B = 0$ yields $\partial B_x / \partial z = \partial B_z / \partial x$. Thus using this to extrapolate yields

$$B_{i,j,0}^x = B_{i,j,2}^x - 2\Delta z \cdot \frac{B_{i+1,j,1}^z - B_{i-1,j,1}^z}{2\Delta x} = B_{i,j,2}^x - \Delta z \cdot \frac{B_{i+1,j,1}^z - B_{i-1,j,1}^z}{\Delta x} \quad (1)$$

using central differences (2nd order) in the x and z derivation (if at the border of the domain, a one-sided derivation is used).

2. B_{ij0}^y : Similar to B_{ij0}^x , we use the x -component of $\nabla \times B = 0$

$$B_{i,j,0}^y = B_{i,j,2}^y - \Delta z \cdot \frac{B_{i,j+1,1}^z - B_{i,j-1,1}^z}{\Delta y} \quad (2)$$

3. B_{ij0}^z : Here only the divergence-free nature is of help, i.e., using $\nabla \cdot B = 0$ yields $\partial B_z / \partial z = -\partial B_x / \partial x - \partial B_y / \partial y$. Finally this leads to

$$B_{i,j,0}^z = B_{i,j,2}^z + \Delta z \cdot \left(\frac{B_{i+1,j,1}^x - B_{i-1,j,1}^x}{\Delta x} + \frac{B_{i,j+1,1}^y - B_{i,j-1,1}^y}{\Delta y} \right) \quad (3)$$

Assuming a uniform permeability μ throughout the measurement area, formulas above hold for the H-field as well, given that $B = \mu H$.

3 Provision of the rational why the determination of the psSAR1g by DASY8/6 Module WPT V2.6+ should be exempted from NUMSIM PAG

IT'IS will provide the rational why the determination of psSAR1g is the standardized flat phantom using the measured incident H-field should be considered a reconstruction method. The implementation does not require any input from the user nor any parameter settings, and therefore should be exempted from the NUMSIM PAG.

The following workflow has been implemented in DASY8/6 Module WPT V2.6+ and would be automatically executed (after a click by the customer to start it):

1. Reconstruct the H-field at the probe surface using the curl- and divergence-free assumptions (see section 2)
2. Reconstruct the vector potential (i.e., A-field) using the H-field measured and reconstructed (see section 3.2)
3. Solve the induced scalar potential ϕ with $\nabla \cdot \sigma \nabla \phi = -j\omega \nabla \cdot \sigma A$ using the finite element technique (FEM) with linear nodal elements and no-flux boundary conditions (ω is the angular frequency, σ the conductivity of the standardized homogeneous phantom ($\sigma = 0.75 \text{ S/m}$, $\rho = 1000 \text{ kg/m}^3$)).
4. Compute the induced E-fields with $E = -j\omega A - \nabla \phi$. The gradient $\nabla \phi$ is computed via FEM's element function's derivation and evaluated at the cell's center.
5. Compute psSAR1g based on the induced E-field via growing around each cell a cube containing $s = \sqrt[3]{1g/\rho}$ where ρ is the mass density (straight forward due to the simple geometry of a lossy half-space). The local SAR distribution is numerically integration within that 1g volume and the maximum value is reported.

3.1 Formula to Reconstruct the Vector Potential A based on the H-field

The vector potential reconstruction finds a vector potential \vec{A} based on the magnetic flux density \vec{B} , i.e., fulfilling $\vec{A} = \nabla \times \vec{B}$. Fortunately, thanks to the work of Laakso *et al.* [1], there exists an explicit formula to compute an ungauged \vec{A} by simply evaluating the formula. This formula reads for the x component A_x :

$$A_x(x, y, z) = - \int_{y_0}^y \left[\frac{1}{3} B_z(x, y', z) + \frac{1}{6} B_z(x, y', z_0) \right] dy' + \int_{z_0}^z \left[\frac{1}{3} B_y(x, y, z') + \frac{1}{6} B_y(x, y_0, z') \right] dz' \quad (4)$$

where x_0 , y_0 and z_0 is an arbitrary point within the domain. The other components can be derived by cyclic permutations. See also the original paper [1], where the formula for all components are written down for $x_0 = 0$, $y_0 = 0$, $z_0 = 0$. The path integrals are numerically evaluated, i.e., using any quadrature scheme in text books (i.e., the path integral becomes a sum of weighted measurement values). Laakso proofs mathematically [1], that the equation fulfills the curl relation $\vec{A} = \nabla \times \vec{B}$.

In its discretized form (measurements on a rectilinear lattice) this formula boils down to a weighted sum.

3.2 Uncertainty for psSAR1g

All steps have been optimized for numerical stability, extensively validated and the uncertainty for psSAR1g assessed to be $<33.9\%$ ($k = 2$). If the measured data do not meet the numerical requirements for assessing of psSAR1g, the workflow is not executed.

Since the user of the system cannot interact with or modify any parameter involved in this workflow, we believe that the determination of psSAR1g by DASY8/6 Module WPT V2.6+ should be exempted from NUMSIM PAG.

4 Conclusions

We have provided additional information to clarify:

- the incident H-field reconstruction at the surface of the probe, and
- determination of the psSAR1g induced in the standardized infinite flat phantom in DASY8/6 Module WPT V2.6+.

We also removed the misleading term "Sim4Life Plug-In" from the manual as all functions are integral parts of DASY8/6 Module WPT V2.6+, and users cannot interact with or modify any parameter involved in these optimized and validated reconstructions, i.e., the only input is the measured field data. In view of this, we believe that the determination of the surface fields and psSAR1g by DASY8/6 Module WPT V2.6+ should be exempted from NUMSIM PAG.

References

- [1] Ilkka Laakso, et al., *Modelling of induced electric fields based on incompletely known magnetic fields*, Phys. Med. Biol., 62, 6567-6587, 2017.